



THE SIMULATION OF ELASTIC WAVES MOTION ALONG PIPELINES. A SHORT REVIEW

Iulian GIRIP

Romanian Academy, Institute of Solid Mechanics, Ctin Mille 15,
Bucharest, Romania, e-mail: iuliangirip@gmail.com

Abstract This paper is a review of ultrasonic technique which is an efficient tool for nondestructive inspection of pipelines. Quantitative detection and evaluation of flaws of different size and geometry, present in pipelines such as corrosion and cracks need extensive examination of ultrasonic wave propagation phenomena. Horizontally polarized shear waves are known as Lamb waves. These waves are useful in the inspection of the ultrasonic type, since they can be detected on the outer and inner surface of the pipelines. The simulation is relatively easy in straight pipelines but much harder for other geometries which are including curvatures, joints, etc. The goal of the present contribution is to apply two simulation techniques to analyze the wave propagation in pipelines. We discuss the curvilinear elastodynamic finite integration technique (CEFIT) and the local interaction simulation approach (LISA), developed by Schubert and Delsanto, respectively. The two techniques are reviewed in the next sections with examples of their applications.

Key words: Lamb waves, pipelines, LISA, CEFIT.

1. INTRODUCTIONS

The review of this topic uses in principle two relevant papers:

Delsanto, P.P., Schubert, F., Prevorovsky, Z., I. Genesio, I., Chiroiu, C., *CEFIT and LISA simulations of the propagation of elastic waves along pipelines*, Politecnico di Torino. Internal report, and

Agostini, V., Baboux, Jean-C., Delsanto, P.P., Monnier, T., Olivero, D., *Application of Lamb Waves for the Characterization of Composite Plates*, AIP Conference Proceedings **497**, 455 (1999); <https://doi.org/10.1063/1.1302041>.

The oil and petro-chemical industries work with hundreds of kilometres of pipelines. Part failures on gas and oil pipelines have emphasized the need for a reliable non-destructive inspection technique for detecting and locating the flaws in pipelines is needed because high portions of them are insulated and exposed to external corrosion which cannot be easily detected. Modern ultrasonic techniques like the acoustic emission and acousto-elastic methods, are capable to reveal defects in pipelines prior to failure. The cylindrical Lamb waves [1, 2] is a very good solution to the problem of flaws detection and evaluation in pipelines.

A high-energy source may be the pulse laser operating at different energy modes may be considered. The laser-ultrasonic technique is of great potential for a wide range of ultrasonic measurements [3]. The advantage of this technique consists in remote non-contact and well reproducible broadband excitation of structures. By different thermo-elastic or optical absorption by tube surface, different modes of Lamb waves can be obtained. The optical lenses and beam splitters are also good to create various source radiation designs. Suitable coatings may enhance the

absorption of optical energy on the tube surface.

Propagating ultrasonic waves are detected either by direct surface-contact sensors (piezoelectric ultrasonic or acoustic emission probes are mostly used) or by generally less sensitive non-contact sensing devices (e.g. EMAT or laser interferometer). The laser interferometer detection is neither influenced by resonant and directional behavior of sensors, nor by acoustic coupling problems present with piezoelectric transducers (air-coupled piezoelectric transducers are also available at present time). The detected signals are recorded by digital transient recorders with high sampling rates.

To compare numerical wave propagation simulations with experimental observations, laser-ultrasonic excitations of steel tube samples have been realized. Laser interferometer and piezoelectric sensors were used to detect surface displacements and velocities induced at various distances from the ultrasonic wave source.

The elastodynamic finite integration technique for waves in cylindrical geometries (CEFIT) was analysed in [4]. Lamb waves can propagate for a long distance under insulation and may be excited and received using transducers placed at accessible locations, where only small portion of the insulation must be removed [5-8]. Numerical modelling of elastic wave propagation in random particulate composites is analysed in [9]. In [10] the modelling of linear and nonlinear elastic wave propagation using finite integration techniques in Cartesian and curvilinear coordinates is derived, while the method CEFIT - A Numerical Modelling Tool for Axisymmetric Wave Propagation in Cylindrical Media are discussed in [11, 12].

All non-destructive inspection techniques require simple experimental set-ups consisting of an ultrasonic transmitter, receiver, and a device for recording. Nevertheless, the interpretation of the received signal requires a very careful and sophisticated signal processing procedure along with a deep understanding of complex elastic wave propagation mechanisms. A comparison of reliable numerical simulations with appropriate experimental results yields the best way to improve pipeline inspection techniques. The generation and receiving of ultrasonic waves are made by a pair of direct contact longitudinal, shear or Rayleigh wave probes. Simulation of ultrasonic pulse propagation in complex media is presented in [13].

Ultrasonic technique is an efficient tool for nondestructive inspection of pipelines. Quantitative detection and evaluation of flaws of different size and geometry, present in pipelines such as corrosion and cracks need extensive examination of ultrasonic wave propagation phenomena. Horizontally polarized shear waves are known as Lamb waves. These waves are useful in the inspection of the ultrasonic type, since they can be detected on the outer and inner surface of the pipelines. The simulation is relatively easy in straight pipelines but much harder for other geometries which are including curvatures, joints, etc. [14-19]. The goal of the present contribution is to apply two simulation techniques to analyze the wave propagation in pipelines. We discuss the curvilinear elastodynamic finite integration technique (CEFIT) and the local interaction simulation approach (LISA), developed by Schubert and Delsanto, respectively. The two techniques are reviewed in the next sections with examples of their applications.

The goal of the present contribution is to illustrate the applicability of two different simulation techniques to investigate wave propagation mechanisms in pipelines, i.e. the curvilinear elastodynamic finite integration technique (CEFIT) and the local interaction simulation approach (LISA), developed by Delsanto et al. [5-7] and Schubert et al. [4, 11-14], respectively. The two techniques are briefly reviewed in the next two sections.

2. CURVILINEAR ELASTODYNAMIC FINITE INTEGRATION TECHNIQUE (CEFIT)

This section is written in the spirit of the Delsanto et al. work [5-7] The Elastodynamic Finite Integration Technique (EFIT) is scheme to model the elastic wave motion in the numerical time domain for different structures. The method EFIT relies on the approximated evaluation of the

Cauchy's equation of motion in integral form for a linear elastic, isotropic, and non-dissipative medium

$$\iiint_V \rho_0 v(r,t) dV = \iint_S n T(r,t) dS + \iiint_V f(r,t) dV, \quad (1)$$

and the deformation rate equation obtained by derivation of Hooke's law with respect to time

$$\iiint_V T(r,t) dV = \iint_S \lambda I n \cdot v(r,t) + \mu \{n v(r,t) + v(r,t)n\} dS, \quad (2)$$

where $v(r,t)$ is the particle velocity vector, $T(r,t)$ the stress tensor and $\lambda(r)$ and $\mu(r)$ are the Lamé's material constants. I denotes the unity tensor, n the outward normal unit vector on S , and $f(r,t)$ is the density of the volume force. Both equations (1) and (2) are written in integral form. The EFIT procedure consists in a discretized version of the motion equations (1) and (2) which are numerically solved by an explicit time domain scheme on a staggered grid. In comparison with traditional finite difference formulations, EFIT proves a superior treatment of the boundary conditions and stability concerning the numerical treatment.

EFIT was exclusively used only for a Cartesian cubic grid formulation. For modeling the wave motion in pipelines, the Cartesian EFIT is inadequate due to poor discretization of curved surfaces. To avoid this, the discretization used for the cylindrical EFIT scheme is shown in Fig.1, together with the location of the elastic field components on the staggered grid. So, the

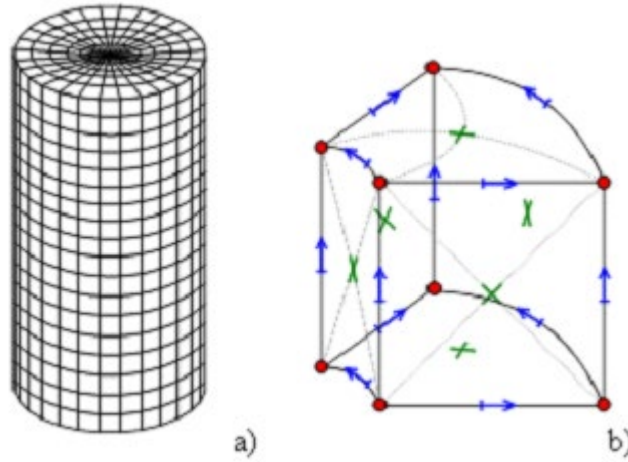


Fig. 1: CEFIT discretization in cylindrical coordinates used for elastic wave modeling in pipeline structures. The arrows, dots and crosses in the figure denote the location of the elastic field components, i.e. particle velocity and stress tensor components [17, 18].

EFIT method is abbreviated as CEFIT is cylindrical or curvilinear EFIT, where C means either cylindrical or curvilinear EFIT. The pipeline model is shown in Fig. 2.

It consists of a cylindrical shell with various kinds of cracks. The cracks may be circumferential or non-circumferential. For circumferential crack with axisymmetric ring source, a 2D method is used.

For non-circumferential cracks and/or non-axisymmetric sources like point impacts, the 3D CEFIT method is necessary.

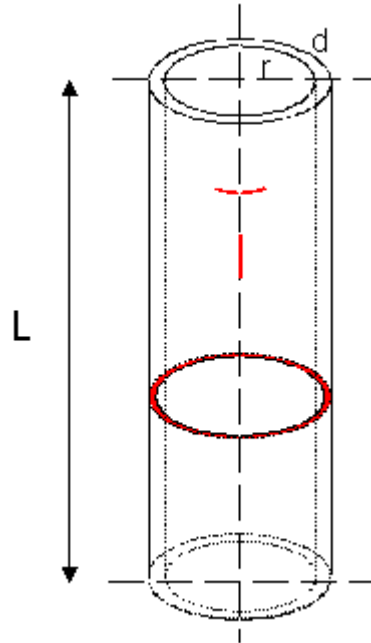


Fig. 2: Straight pipeline geometry including circumferential and non-circumferential cracks in a cylindrical shell environment [17, 18].

For pipelines, the cylindrical and toroidal coordinates can be combined in order to discretize both, the straight as well as the curved parts of the pipeline accurately. Fig.3 shows the cross-sections of 3D-CEFIT models of a pipeline curvature (left hand side) and a joint (right hand side).

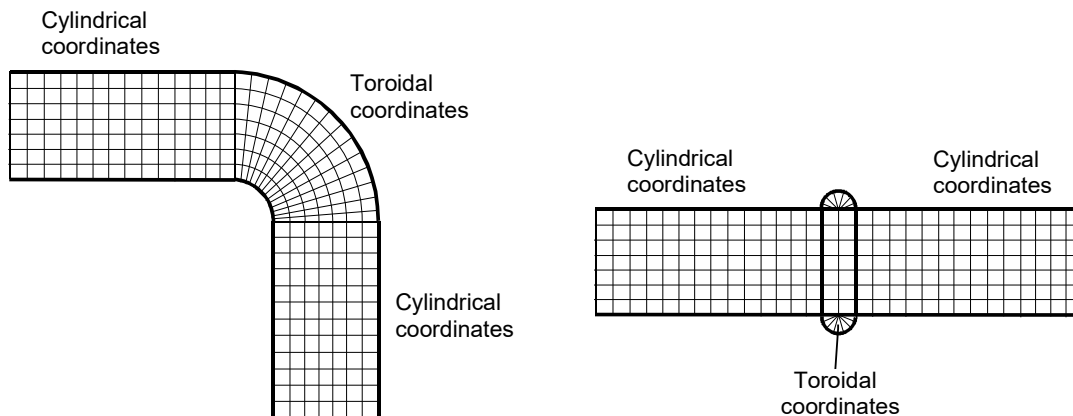


Fig. 3: Cross-sections of 3D-CEFIT models of a pipeline curvature (left hand side) and a joint (right hand side) [17, 18].

For an unfaulted plate, Fig.4 shows a snapshot at time $t=2\mu\text{s}$ of the perpendicular injection at frequency $\nu = 100\text{ kHz}$. To put into evidence the effects of wave propagation, the gray map of each snapshot are re-scaled between the maximum (darkest tone) and the minimum (lightest tone) of the displacements. Fig. 5 shows a snapshot of the longitudinal displacements at time $t=267\mu\text{s}$: the anti-symmetric profile of the displacements reveals the presence of the A_0 Lamb mode. The S_0 mode is also present but, to a much lesser extent.

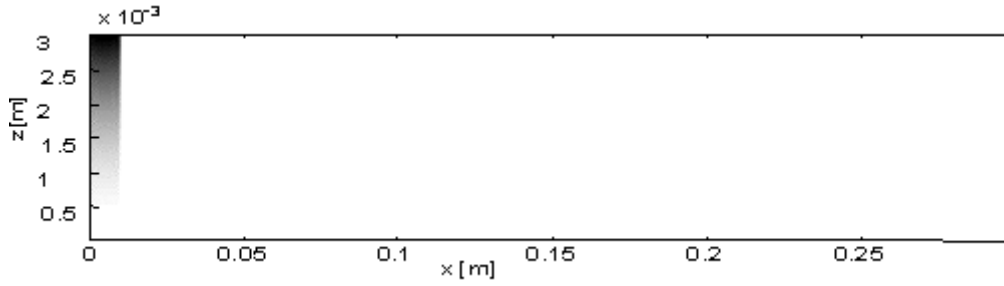


Fig. 4: Snapshot of the injected perpendicular displacements pulse at $t = 2 \mu\text{s}$ [17, 18].



Fig. 5: Snapshot of the displacements amplitude (longitudinal component) at $t = 267 \mu\text{s}$: the A_0 mode is selected [17, 18].

For a CEFIT simulation, we firstly consider the Delsanto example [5-7] of interaction of a quasi-longitudinal wave (center frequency 300 kHz) with a 1.5 mm deep circumferential crack in the outer pipeline wall at $z = 25$ cm. The interaction of a quasi-longitudinal wave with a circumferential crack in the outer pipeline wall is shown in Fig. 6.

Fig. 5 shows the wave propagation in the cross-section of the wall after the incident wave arrives at the crack. A quasi-longitudinal and a flexural wave, both running in forward as well as in backward direction are observed. The time signals on the right show the velocity components v_z calculated at the top, and v_r calculated to the bottom. Both pulses are detected at the outer pipeline wall at $z = 15$ cm. The incident wave arrives at the time $t \approx 27 \mu\text{s}$ while the reflected waves can be observed at $t \approx 65 \mu\text{s}$ and $t \approx 80 \mu\text{s}$, respectively. Fig. 6 shows the velocity components v_z at the top, and v_r at the bottom.

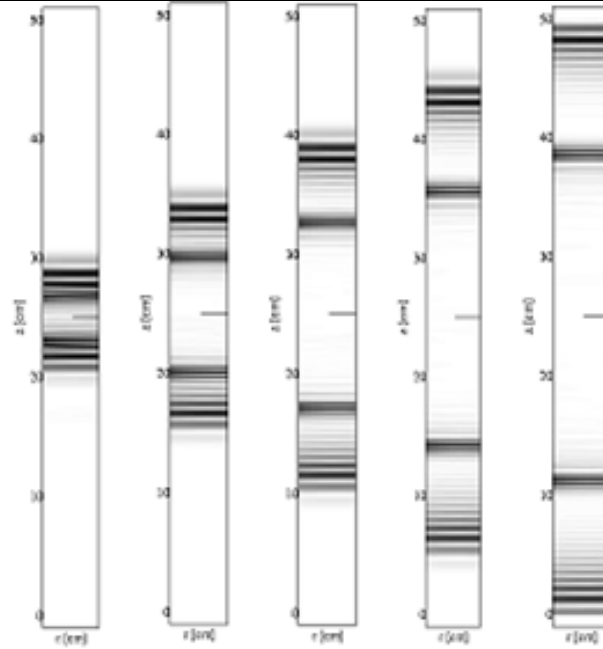


Fig. 6: CEFIT simulation of interaction of a quasi-longitudinal wave (center frequency 300 kHz) with a 1.5 mm deep circumferential crack in the outer pipeline wall at $z = 25$ cm [17, 18].

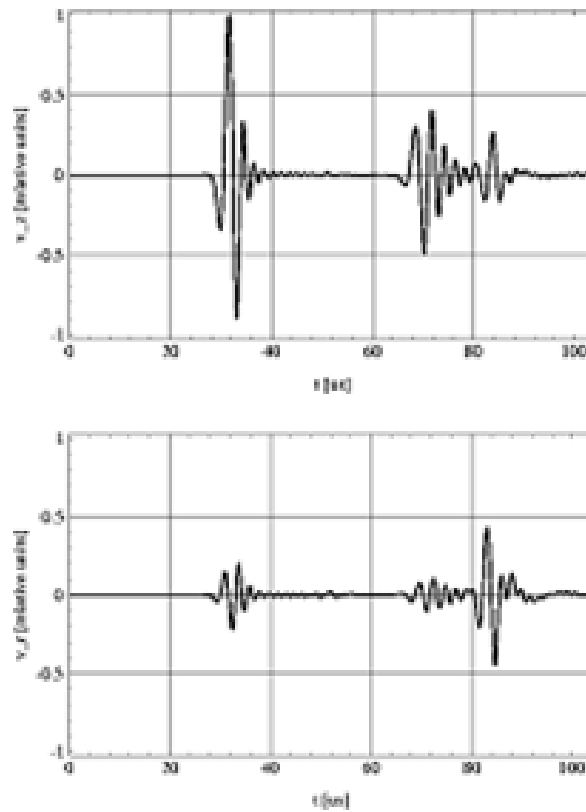


Fig. 7: Velocity components v_z at the top, and v_r at the bottom [17, 18].

Interaction of a quasi-longitudinal wave with a horizontal and a vertical oriented non-circumferential crack in the inner pipeline wall is shown in Fig. 7.

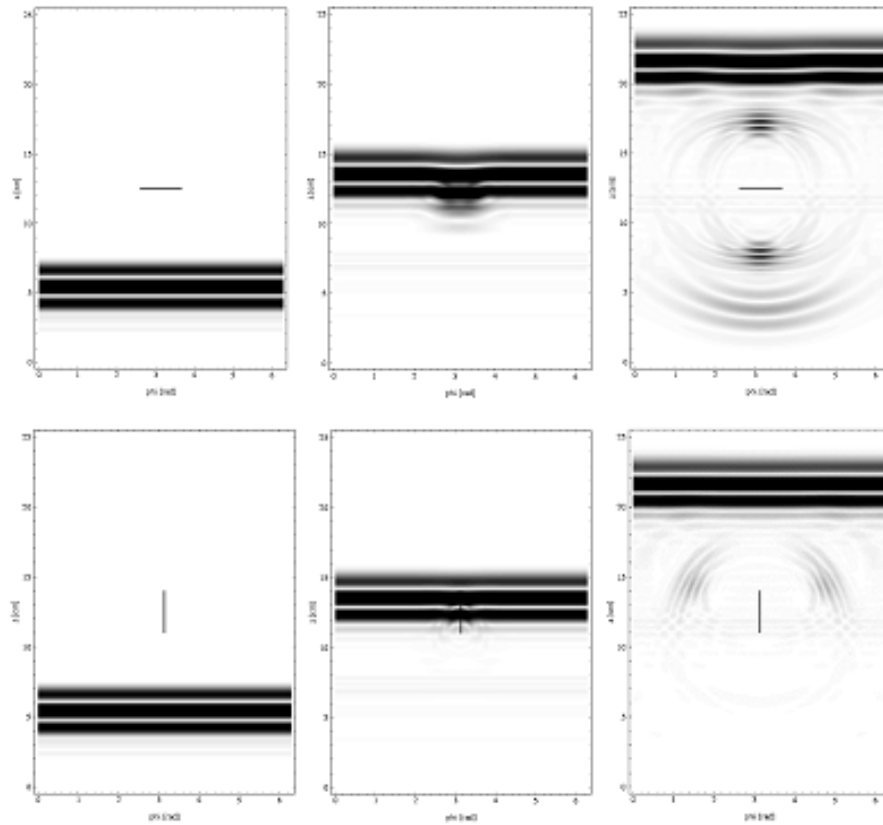


Fig. 8: 3D-CEFIT simulation of interaction of a quasi-longitudinal wave (center frequency 200 kHz) with a horizontal (top) and vertical (bottom) oriented 3 cm long non-circumferential crack in the inner pipeline wall [17, 18].

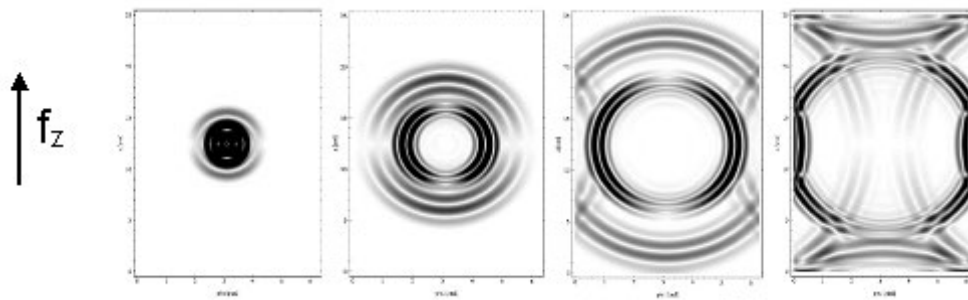


Fig. 9: 3D-CEFIT simulation of wave propagation due to elementary point impact on the pipeline wall. The figure shows the elastic wave field caused by horizontal force impact producing a quasi-longitudinal wave as well as a pure shear wave [17, 18].

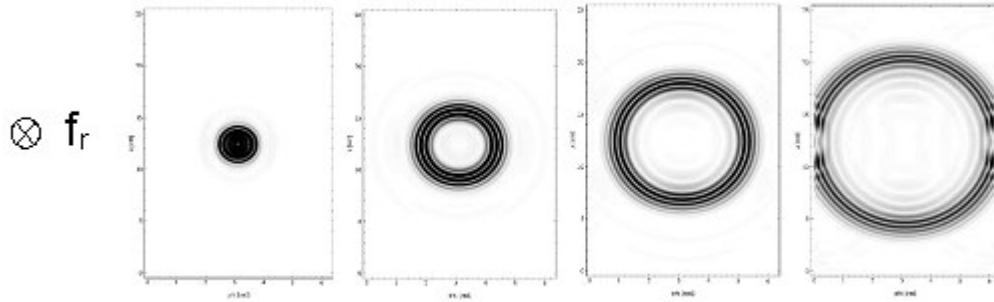


Fig. 10: 3D-CEFIT simulation of wave propagation due to elementary point impact on the pipeline wall (φz -plots of the outer cylindrical shell surface). The figure shows the wave field produced by radial force impact as can be realized by a pencil break for example. In this case a flexural wave is generated [17, 18].

3. LOCAL INTERACTION SIMULATION APPROACH (LISA)

The simulation of the ultrasonic wave propagation in both homogeneous and heterogeneous media is possible if we derive heuristically the iteration equations by means of a simple Spring Model [14]. In the model, the specimen is first discretized with gridpoints representing tiny homogeneous cells of materials. Across the gridpoints a network of springs is assumed, to ensure an elastic behaviour inside each material component and, in the case of perfect contact interfaces, a perfect contact among different components. Fig. 11 gives a pictorial representation of the Spring Model, in the case of a homogeneous material, by depicting the interaction of a generic grid point O with its nearest neighbors, labelled with integers from 1 to 8.

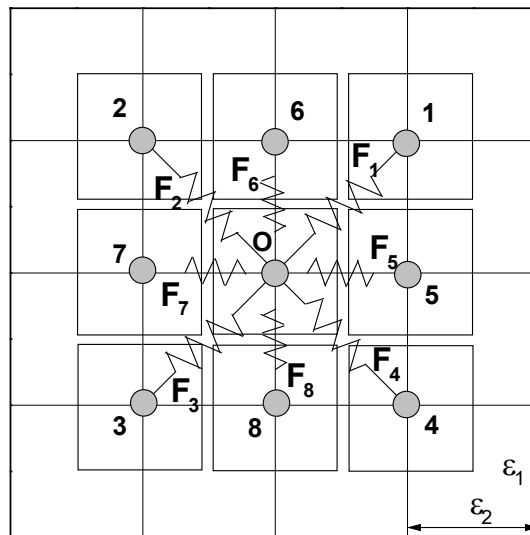


Fig. 11: Spring Model for a generic gridpoint O in the case of a homogeneous material [17, 18].

If the gridpoint O location is on the interface between different materials at the right and left of the vertical through O , then the two vertical springs (F_6 and F_8) are each split into two separate springs, according to the physical properties of the corresponding material. If O is a crosspoint at the intersection of two orthogonal interfaces separating four different materials, then all four horizontal and vertical springs are split each into two springs. In this way, we obtain the iteration equations for the displacements of a pulse propagating into a heterogeneous discretized medium.

We remind that the medium can be arbitrarily complex, since each grid point may be a cross point.

The further step models the interface contact by means of additional springs. The node point O is then split into four subnodes O_1, O_2, O_3 and O_4 , connected through internal springs (Fig.12).

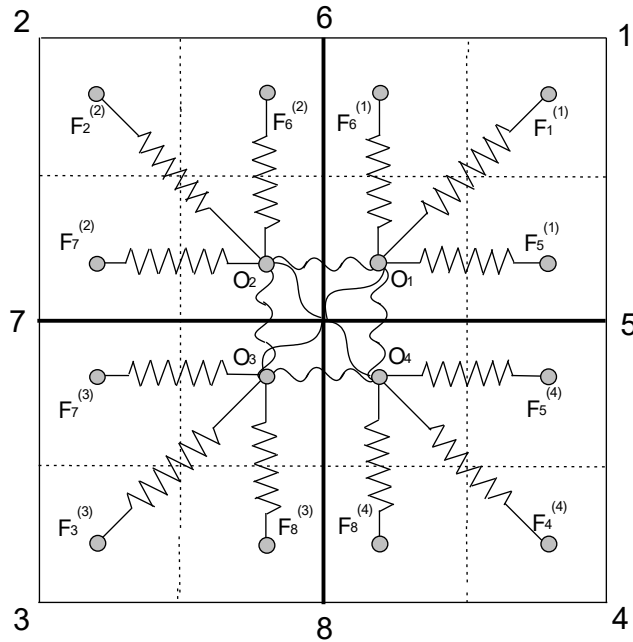


Fig. 12: Spring Model for a heterogeneous material [17, 18].

Each node may be characterized by a contact quality tensor Q_{ij} in order to introduce the possibility of weakened or broken springs. If $Q_{ij} = 0$, the bond at the corresponding node is considered perfect. A smaller or zero value for any component of Q_{ij} indicates possible interface flaws (Fig. 13).

In fig.13, the Intact springs are marked with a solid line ($Q_{ij} = 1$), broken springs with a dotted line ($Q_{ij} = 0$) and weaken springs with a solid dashed line ($Q_{ij} = 0.5$).

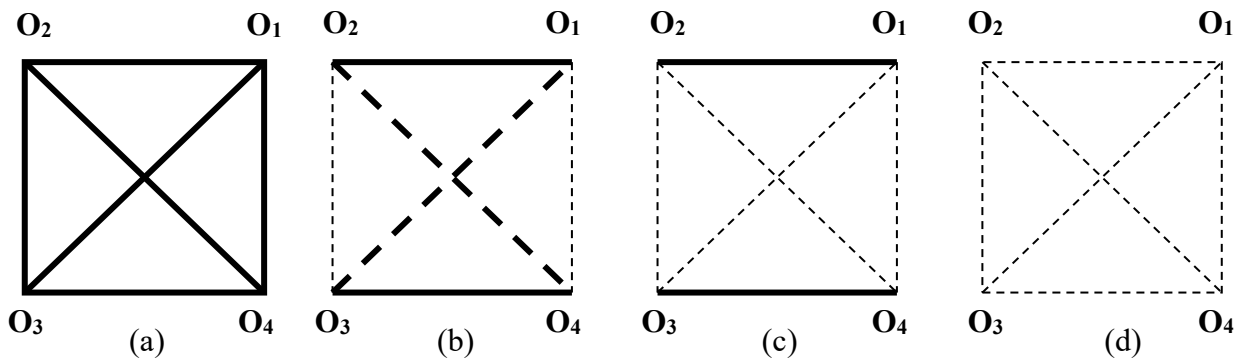


Fig. 13: Sets of internal springs; a) Intact springs are marked with a solid line ($Q_{ij} = 1$); b) broken springs with a dotted line ($Q_{ij} = 0$) and c) weaken springs with a solid dashed line ($Q_{ij} = 0.5$) [17, 18].

4. RESULTS AND CONCLUSIONS

We analyze in this section the effects of various kinds of flaws in the pipeline (see Fig. 14), These flaws are defined as gridpoints in which some of the components of the contact quality tensor Q_{ij} are different from 1 [16]. In order to separate them from other reflection or mode-conversion effects, we have considered the propagation of a longitudinal ultrasonic wave in a homogeneous plate, discretized by means of a 350 times 300 grid. An imperfection has been introduced at $i = 150$ and $j = 148, 149, 150, 151, 152$ and the wave has been injected from the left side of the specimen.

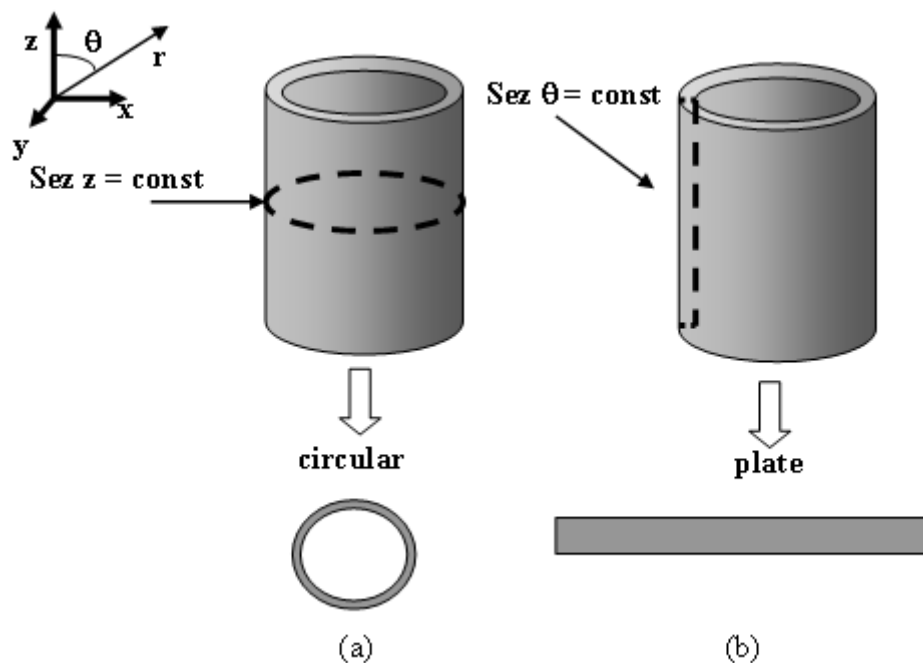


Fig. 14 : Transversal (a) and longitudinal (b) sections of the pipeline [17, 18].

In the particular case only three kinds of flaws are significantly different due to the symmetry of the problem. A completely arbitrary flaw may be seen as a combination of these three basic types.

For a 350 x 300 grid, we introduce an imperfection at $i = 150$ and $j = 148, 149, 150, 151, 152$. The wave has been injected from the left side of the plate. In the particular case under consideration, due to the symmetry of the problem, only three kinds of flaws are significantly different:

1. vertical defect, defined by $Q_{12} = Q_{13} = Q_{24} = Q_{34} = 0$;
2. vertical slippage, defined e.g. by $Q_{12} = 0$;
3. rhomboidal slippage, defined e.g. by $Q_{13} = 0$.

For a completely arbitrary flaw may be seen as a combination of these three types.

All the other components of Q_{ij} are, in the three cases, equal to 1. Since the defect is small, the incident longitudinal wave propagates almost undisturbed. A reflected wave is also quite noticeable, since it reaches an amplitude of almost 20% that of the incident wave. In fact, a defect behaves as a source of almost symmetrical spherical waves, which create a quite conspicuous interference pattern. In addition, there is generation, by mode conversion, of shear waves of opposite sign between top and bottom, accompanied by reconversion to longitudinal modes, since the tips of the defects behave as point sources of shear waves. The behaviour of the reflected wave

is in good qualitative agreement with experimental data.

We see that the incident plane wave propagates almost undisturbed, with a noticeable, but much smaller reflected wave (about 4% of the incident wave) and a generation by mode conversion of shear waves. The strong anisotropy of the problem is clearly visible, particularly in the bottom plots, where a vertical shift of the two spherical waves generated by the tips of the flaw is evident, with opposite signs of the amplitude of the mode converted shear waves.

In the case of a rhomboidal slippage, the results are similar to those obtained before, but with an even stronger anisotropy effect. The wave front is no longer quasi-spherical and the propagation direction of the generated waves, once they are far enough from the defect, is clearly in a diagonal upwards direction. Again, the reflected wave has an amplitude of a few per cent of the incident wave.

To conclude, we wish also to present an illustration of Lamb waves propagation in a transversal cut of the pipeline. Fig. 15 represents the case of an unblemished section. Cases with different kinds of defects can be easily modeled and analyzed, following the procedure described for the case of longitudinal cuts.

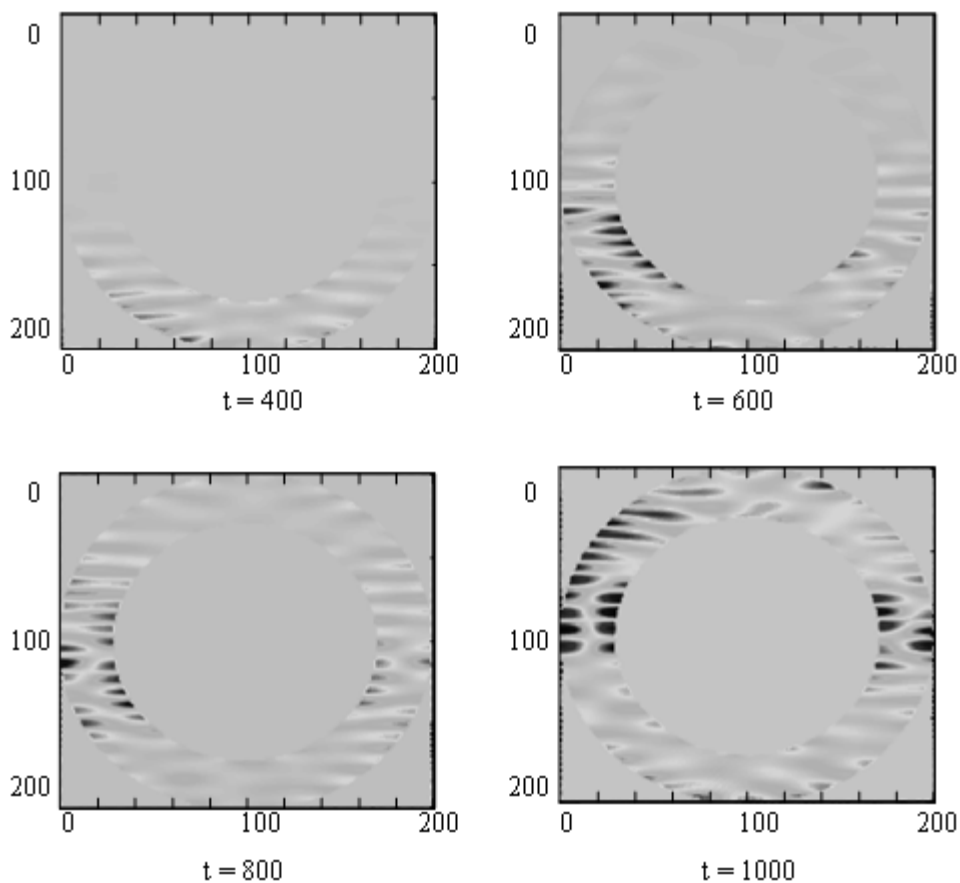


Fig. 15: Snapshots at various times of the amplitude of a low frequency Lamb mode in a circular section of a pipeline [17, 18].

Acknowledgments. This work was supported by a grant of the Romanian Ministry of Research and Innovation, CCCDI-UEFISCDI, project number PN-III-P2-2.1-PED-2019-0085 CONTRACT 447PED/2020

REFERENCES

1. LOWE, M.J.S., ALLEYNE, D.N., CAWLEY, P., *Defect detection in pipes using guided waves*, Ultrasonics, **36**(1-5), pp. 147-154, 1998.
2. THOMPSON, D.O., CHIMENTI, D.E., eds.: *Review of Progress in Quantitative NDE*, vol. **16**, Plenum Press, New York, 1997.
3. SCRUBY, C.B., DRAIN, L.E., *Laser Ultrasonics Techniques and their Applications*, Hilger, Bristol, 1990.
4. SCHUBERT, F., PEIFFER, A., KOEHLER, B., SANDERSON, T., *The Elastodynamic Finite Integration Technique for Waves in Cylindrical Geometries (CEFIT)*, J. Acoust. Soc. Am., **104** (5), 1998.
5. DELSANTO, P.P., IORDACHE, D., IORDACHE, C., RUFFINO, E., *Analysis of stability and convergence in FD simulations of 1D ultrasonic wave propagation*, Mathl. Comput. Modelling **25** (6), pp. 19-29, 1997.
6. DELSANTO, P.P., WHITCOMBE, T., CHASKELIS, H.H., MIGNOGNA, R.B., *Connection machine simulation of ultrasonic wave propagation in materials. I: the one-dimensional case*, Wave Motion, **16** (1), pp. 65-80, 1992.
7. DELSANTO, P.P., SCHECHTER, R.S., CHASKELIS, H.H., MIGNOGNA, R.B., KLINE, R., *Connection machine simulation of ultrasonic wave propagation in materials-II: The two-dimensional case*, Wave Motion, **20**, pp. 295-314, 1994.
8. FELLINGER, P., MARKLEIN, R., LANGENBERG, K. J., KLAHOLZ, S., *Numerical modeling of elastic wave propagation and scattering with EFIT - elastodynamic finite integration technique*, Wave Motion, **21**, pp. 47-66, 1995.
9. MARKLEIN, R., BAERMANN, R., LANGENBERG, K. J., *The ultrasonic modeling code EFIT as applied to inhomogeneous dissipative isotropic and anisotropic media*, In: *Review of Progress in Quantitative Nondestructive Evaluation (QNDE)*, Vol. 14, Plenum Press, New York, pp. 251-258, 1995.
10. LANGENBERG, K. J., HANNEMANN, R., KACZOROWSKI, T., MARKLEIN, R., KOEHLER, B., SCHURIG, C., WALTE, F., *Application of modeling techniques for ultrasonic austenitic weld inspection*, *NDT&E International*, **33**, pp. 465-480, 2000.
11. SCHUBERT, F., KOEHLER, B., *Numerical modeling of elastic wave propagation in random particulate composites*, In: *Nondestructive Characterization of Materials VIII*, Plenum Press, New York, pp. 567-574, 1998.
12. SCHUBERT, F., KÖHLER, B., *Modeling of linear and nonlinear elastic wave propagation using finite integration techniques in Cartesian and curvilinear coordinates*, In: *Proc. EUROMECH 419 colloquium 'Elastic Waves in Nondestructive Testing'*, October 2000, Prague, Czech Republic, 2000.
13. SCHUBERT, F., PEIFFER, A., KOEHLER, B., *CEFIT - A Numerical Modeling Tool for Axisymmetric Wave Propagation in Cylindrical Media*, In: *Review of Progress in Quantitative Nondestructive Evaluation (QNDE)*, Vol. 18A, Plenum Press, New York, pp. 95-102, 1998.
14. SCHUBERT, F., KOEHLER, B., *Time Domain Modeling of Axisymmetric Wave Propagation in Isotropic Elastic Media with CEFIT - Cylindrical Elastodynamic Finite Integration Technique*, accepted for publication in *Journal of Computational Acoustics (JCA)*, presented at ICTCA' 99, The 4th International Conference on Theoretical and Computational Acoustics, May 1999, Trieste, Italy.
15. STĂNESCU, N.D., PANDREA, N., *Dynamics of a Rigid with Many Points Situated on Fixed Surfaces by a Multibody Approach*, *Romanian Journal of Mechanics*, **1** (1), pp. 21-39, 2016.
16. BRATU, P., MUNTEANU, L., *Applications of the perpetual points in dynamics*, *Romanian Journal of Mechanics*, **3** (1), pp. 27-38, 2018.
17. DELSANTO, P.P., SCHUBERT, F., PREVOROVSKY, Z., GENESIO, I., CHIROIU, C., *CEFIT and LISA simulations of the propagation of elastic waves along pipelines*, Politecnico di Torino. Internal report,
18. AGOSTINI, V., BABOUX, Jean-C., DELSANTO, P. P., MONNIER, Th., OLIVERO, D., *Application of Lamb Waves for the Characterization of Composite Plates*, *AIP Conference Proceedings*, **497**, 455 1999; <https://doi.org/10.1063/1.1302041>.
19. VLASE, S., *Finite element analysis of flexible multibody systems. An overview*, *Romanian Journal of Mechanics*, **3** (2), pp. 48-63, 2018.

Received December 22, 2020